Multiscale simulations suggest a mechanism for integrin inside-out activation

Antreas C. Kalli, Iain D. Campbell, and Mark S. P. Sansom[1]

Department of Biochemistry, University of Oxford, South Parks Road, Oxford OX1 3QU, United Kingdom

Edited by Axel T. Brunger, Stanford University, Stanford, CA, and approved June 7, 2011 (received for review March 21, 2011)

Integrins are large cell-surface adhesion receptors that can be activated to a high affinity state by the formation of an intracellular complex between the integrin β-subunit tail, the membrane, and talin. The F2 and F3 subdomains of the talin head play a key role in formation of this complex. Here, activation of the integrin αIIb/β3 dimer by the talin head domain was probed using multiscale molecular dynamics simulations. A number of novel insights emerge from these studies, including (*i*) the importance of the integrin αIIb subunit F992 and F993 residues in stabilizing the "off" state of the αIIb/β3 dimer, (*ii*) a crucial role for negatively charged groups in the F2-F3/membrane interaction, (*iii*) binding of the talin F2-F3 domain to negatively charged lipid headgroups in the membrane induces a reorientation of the β transmembrane (TM) domain, (*iv*) an increase in the tilt angle of the β TM domain relative to the bilayer normal helps to destabilize the α/β TM interaction and promote a scissor-like movement of the integrin TM helices. These results, combined with various published experimental observations, suggest a model for the mechanism of inside-out activation of integrins by talin.

Integrins are heterodimeric (αβ) cell-surface receptors; each subunit contains a large extracellular (ecto) domain, an α-helical transmembrane (TM) domain, and a cytoplasmic domain (1). Integrins are crucial for signal transduction events involved in cell adhesion, migration, and differentiation (2–5). In mammals, combinations of the 18 α and 8 β subunits may form at least 24 different integrins. TM signaling can occur via outside-in (6) and inside-out pathways. In inside-out activation, the cytoplasmic tail of the integrin β subunit forms a complex with a cytoplasmic protein, talin, at the membrane surface (7–14).

Talin consists of a flexible rod and a globular head that has four subdomains (F0 to F3) (15, 16). The F3 subdomain alone is sufficient for αIIbβ3 integrin activation (17), but interactions between a positively charged patch in the F2 surface (14, 18) and negatively charged groups in the membrane are also crucial for integrin activation and clustering (19). Structural and functional studies suggest that the F0-F1 subdomain also contributes to the activating membrane complex (16, 20), partly via a flexible loop in the F1 domain. PIP_2 is also believed to play a role (19).

The inactive state of integrins is maintained by intersubunit associations in the TM (21–26) and cytoplasmic regions (27–29) of the two integrin subunits. Integrin activation is believed to involve dissociation or destabilization of the two integrin TM helices (29–33), followed by rearrangement of the ectodomain to an extended conformation (34–37). Recent NMR and modeling studies (24) revealed similar structures for the αIIb and β3 TM helices in a membrane-like environment. Two main interaction surfaces between the two TM helices of the αIIb/β3 complex were identified in the NMR structure. These were called an outer membrane clasp (OMC), in which close packing of the helices is facilitated by a Gx_3G motif in αIIb, and an inner membrane clasp (IMC), which involves interactions of F992 and F993 in αIIb with the β3 tail together with a salt bridge between αIIbR995 and β3D723 (24).

Different models have been proposed for structural changes in the membrane region during activation, including "piston" and "scissors" movements of the TM helices (38). However, more recent studies (7, 23, 29, 32, 39, 40) have been interpreted in terms of a model in which the binding of talin to the integrin β cytoplasmic tail and the TM domain disrupts the OMC and IMC interactions between the two TM helices, leading to helix separation and subsequent switching of the integrins to a high affinity state (14). Resolution of the underlying mechanism of activation thus requires information about the conformational dynamics of integrin/talin/membrane interactions that is not readily available from experimental methods.

Molecular dynamics (MD) simulations (41) can play a key role in understanding the dynamic interactions of membrane proteins with their environment (42). They have been used to investigate the interactions of TM helices with one another in a bilayer environment (43) as well as the interactions of peripheral proteins with membranes (44–47). MD studies of the F2-F3 domain of talin (18) in a bilayer demonstrated a key role for electrostatic interactions between the protein and anionic lipid headgroups.

Here, we use a multiscale MD simulation approach (48, 49) to explore the conformational dynamics of the interaction of the integrin TM helix dimer with talin F2-F3 and a lipid bilayer. The aim was to understand the inside-out activation mechanism. On the basis of these studies, we suggest how talin can weaken the α/β TM association and promote an integrin conformation that corresponds to a high affinity state.

Results and Discussion

Conformation and Dynamics of the Integrin αIIb/β3 TM Helix Dimer. As a first step toward understanding how talin interactions may modulate the behavior of the integrin αIIb/β3 TM helix dimer, we simulated the conformational dynamics of the TM helix dimer. We started with the coordinates of the NMR structure [Protein data Bank (PDB) ID code 2K9J], which is probably a reasonable approximation of the low-affinity integrin "off" state. Coarse-grained (CG)-MD simulations were used to optimize the position of the TM helix dimer relative to a palmitoyl-2-oleoyl-sn-glycero-3-phosphocholine/palmitoyl-oleoyl-phosphatidyl glycerol (POPC/POPG) bilayer, while restraining the αIIb TM helix to be perpendicular to the bilayer. This orientation of αIIb is suggested by the NMR structures of the αIIb helix (50) and the αIIb/β3 dimer in bicelles (24). The resultant CG system (i.e., helix dimer plus bilayer) was converted to atomistic resolution (49) to form the starting point for 3×100 ns simulations.

In these αβ1-AT (Table 1) simulations, the TM dimer remained stable (Fig. 1*A*). Both IMC interactions [i.e., the αIIbR995-β3D723R salt bridge and the αIIb(F992,F993)-β3 aromatic cluster interactions] and the OMC interaction, involving the αIIb Gx_3G motif, were maintained throughout all three simulations.

Author contributions: A.C.K., I.D.C., and M.S.P.S. designed research; A.C.K. performed research; A.C.K., I.D.C., and M.S.P.S. analyzed data; and A.C.K., I.D.C., and M.S.P.S. wrote the paper.

The authors declare no conflict of interest.

This article is a PNAS Direct Submission.

Freely available online through the PNAS open access option.

[1]To whom correspondence should be addressed. E-mail: mark.sansom@bioch.ox.ac.uk.

This article contains supporting information online at www.pnas.org/lookup/suppl/doi:10.1073/pnas.1104505108/-/DCSupplemental.

Table 1. Summary of simulations

Simulation	Proteins	Coordinates	Duration, ns
αβ1-AT	αIIb/β3 TM	2K9J	3 × 100
αβ2-AT	αIIb(R995D)/β3 TM		3 × 100
αβ3-AT	αIIb(F992A,F993A)/β3 TM		3 × 100
αβ4-AT	αIIb(F992A,F993A, Δ995-998)/β3 TM		3 × 100
αβ5-AT	αIIb(G972S)/β3 TM		1 × 100
αβ6-AT	αIIb(G976L)/β3 TM		1 × 100
F2F3-AT	talin F2-F3	3G9W	1 × 30
β-AT	β* TM	model based on	3 × 70
β-F3-AT	β* TM/talin F3	2K9J β3 + 3G9W	3 × 70
β-F2F3-AT	β* TM/talin F2-F3		3 × 70
αβ-F2F3-CG	αIIb/β* TM/talin F2-F3	model based on	5 × 5,000
αβ-F2F3c-AT	αIIb/β* TM/talin F2-F3 closed	2K9J + 3G9W	3 × 100
αβ-F2F3p-AT	αIIb/β* TM/talin F2-F3 partial		3 × 100
αβ-F2F3o-AT	αIIb/β* TM/talin F2-F3 open		3 × 100

All simulations were of the protein complex in a POPC/POPG lipid bilayer. System sizes ranged from approximately 40,000 (αβ simulations) to approximately 100,000 (αβ-F2-F3 simulations). β* indicates a chimeric β chain (β3/β1D)—see main text for details.

The tilt angles for the αIIb and the β3 helices during the αβ1-AT simulations were approximately 5 and 30°, respectively, and the helix dimer maintained its right-handed packing with a helix crossing angle of approximately −35° (Fig. 1*C*).

Effect of Mutations on the Stability of the Integrin αIIb/β3 TM Helix Dimer. The two components of the IMC (i.e., the salt bridge and the aromatic cluster) were further explored by simulations of mutants. Thus, in simulation αβ2-AT (Table 1), the αIIbR995D mutation disrupted the salt bridge but did not appear to greatly alter the conformational stability of the dimer, as the hydrophobic interactions of the aromatic cluster of the IMC remained intact, and helix packing in the OMC was not perturbed. Thus, the αIIbR995D mutant dimer retained its right-handed helix packing, with a crossing angle of approximately −35° (Fig. 1*C*) (i.e., similar to the crossing angle for the WT helix dimer). This is in good agreement with experimental results that suggest that disruption of the αIIb R995 and β3 D723 salt bridge weakens, but does not eliminate, the α/β association (24, 51).

The contribution of the aromatic cluster of the IMC to the conformational stability of the αIIb/β3 dimer was also explored by mutation of αIIb (F992A, F993A) in simulation αβ3-AT (Table 1). This double mutation significantly perturbed the packing of the helices, reducing their crossing angle to approximately −10° (Fig. 1*C*). The β3 tilt angle relative to the bilayer normal remained at approximately 30° (i.e., similar to the WT), but the tilt angle of the αIIb helix increased to approximately 20° (compare approximately 5° in the WT). This increase in the tilt angle reflects the change in the packing of the two helices. This change is such that the β3 residues M701 and L705 in the OMC and residues L712 and K716 in the IMC, which interact with the αIIb helix in the WT, no longer form these contacts, resulting in looser packing of the two helices. This is in agreement with mutational data that suggest that substitution of either F992A or F993A activates integrins (30).

In simulation αβ4-AT, both components of the IMC were removed by mutation (as in αβ3-AT) of the aromatic residues and deletion of the salt-bridging arginine of the α subunit. In all three αβ4-AT simulations, the distance between the residue 992, 992 region of αIIb and the β3 helix increased. This altered the packing of the two helices, resulting in a wider distribution of crossing angles. However, disruption of the packing of the OMC clasp was observed only in one out of the three αβ4-AT simulations.

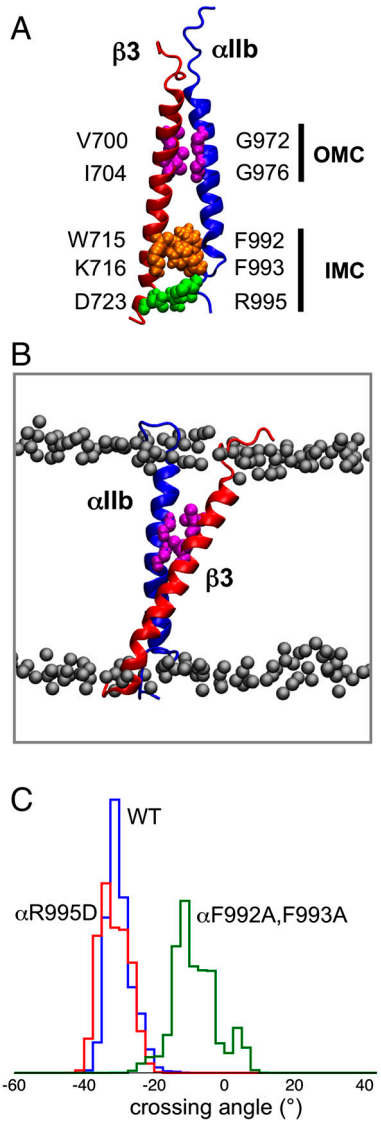

Fig. 1. The αIIbβ3 TM helix dimer. (*A*) Structure of the αIIb (blue) β3 (red) TM helix dimer (PDB ID code 2K9J). Interacting residues in the OMC are in magenta, in the IMC clasp in orange, and the αIIb R995 to β3 D756 salt bridge is in green. (*B*) Snapshot (100 ns) from the αβ1-AT simulation (i.e., WT; see Table 1 for details) showing the two TM helices, the interacting residues of the OMC (magenta), and the phosphorus atoms of the POPC/POPG lipid bilayer (gray). (*C*) Helix crossing angle distributions for the αβ1-AT (blue), αβ2-AT (i.e., αIIbR995D; red), and αβ3-AT (i.e., αIIb F992A,F993A; green) simulations. A negative crossing angle corresponds to right-handed helix packing, a positive angle to left-handed packing.

This suggests that release of the IMC alone may not be sufficient to disrupt all the αIIb/β3 TM interactions.

The OMC is formed by a glycophorin-like interaction (52), involving a Gx_3G motif formed by residues G972 to G976 of the αIIb helix. Mutation of either G972 to serine (αβ5-AT; Table 1) or of G976 to leucine (αβ6-AT) has been reported to induce integrin activation (24, 53), but neither mutation showed significant perturbation of the dimer in our 100-ns atomistic simulations. However, multiscale self-assembly simulations of αIIb/β3 TM helix interactions, using an approach previously tested for glycophorin (43, 54), suggest that mutations of the glycine residues in the OMC do indeed perturb helix packing.

Interactions with Talin Perturb the Integrin TM Helices. We next explored how interactions with the F2-F3 domains of the talin head

modulate the TM helices in a lipid bilayer. If signaling from inside to outside is indeed mediated by a change in packing interactions of the TM helices, then one would anticipate that F2-F3 bilayer interactions (18) could perturb TM/TM and/or TM/bilayer interactions in the simulations. A short (30-ns) atomistic simulation of F2-F3 bound to the PC/PG bilayer revealed a small relative movement (approximately 6°) of the F2 subdomain relative to F3. This movement optimizes contacts with the lipids and is made possible by a flexible linker between the two subdomains. More detailed analysis of F2-F3/lipid contacts confirmed earlier results (18), showing a preference for the F2-F3 domain to interact with negative lipid headgroups.

We next investigated how the close association of the F2-F3 domain with an anionic bilayer might modulate the integrin TM domains, by performing simulations of F3 and of F2-F3 in complex with the β TM helix. The results were compared with the β TM helix alone (β-AT, β-F3-AT, and β-F2F3-AT in Table 1). The β helix was modeled on the structures of the αIIb/β3 TM helix dimer [PDB ID code 2K9J (24)] and of talin F2-F3 bound to the cytoplasmic tail of the integrin β1D [PDB ID code 3G9W (14)]. In the β-F2-F3 simulations, there was a significant increase (approximately 15°) in the tilt angle of the β TM helix relative to that observed in either the β-AT or αβ-AT simulations (Fig. 2). Further analysis of this change revealed no significant movement of the F3 subdomain relative to the β helix. In contrast, the F2 subdomain rotates approximately 10° relative to F3, possibly to optimize the interactions with the bilayer. Examination of H-bonds and close contacts reveals that the F2-F3/bilayer interface in the β-F2F3-AT simulation is similar to that identified in simulations of F2-F3 and bilayer alone. A comparable movement of the β TM helix was seen in the β-F3-AT simulations. Again an increase in β TM helix tilt angle of approximately 15° was seen over the course of the simulation.

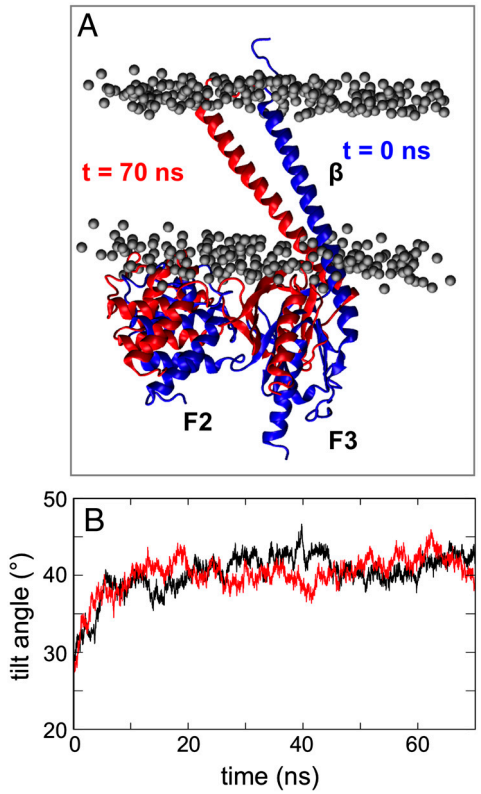

Fig. 2. Tilting of the β3 TM helix in β3/talin simulations. (*A*) Initial (blue) and final ($t = 70$ ns; red) orientation of the F2-F3-β complex in one of the β-F2-F3 simulations. (*B*) The β3 TM helix tilt angle relative to the bilayer normal for β-F2F3-AT (black) and β-F3-AT (red) simulations.

The β TM helix also adopted a similar tilted orientation (approximately 37°) in simulations (β-AT) of just the β TM in a bilayer. Taken together, these three simulations indicate that the β TM helix prefers to adopt a higher tilt angle relative to the bilayer than in the αβ TM dimer. The drive for the β TM helix to a higher tilt angle may arise because the hydrophobic helix length (approximately 40 Å) is better accommodated; the tilted orientation also places the W715 sidechain in the lipid headgroup region and allows the K716 sidechain to interact with lipid phosphate groups. This tendency of the β3 TM helix to adopt a tilted orientation in the membrane is consistent with other studies of integrin TM domains (19, 55). The higher tilt angle of the β TM also allows the talin F2-F3 subdomain to optimize its interactions with the anionic bilayer surface.

Changes in Integrin TM Helix Packing Induced by Talin F2-F3. We next sought to explore the effect of the talin F2-F3 subdomain on TM helix packing and/or the β TM tilt. To do this, the NMR structure of the αIIb/β3 TM helix dimer [PDB ID code 2K9J (24)] and the X-ray structure of F2-F3 in complex with the cytoplasmic tail of integrin β1D [PDB ID code 3G9W (14)] were combined. The backbone coordinates of the helical region of β1D from the F2-F3-β1D structure and the β3 helix from α/β TM dimer structure were aligned. After the alignment, the β3 residues from T720 to F727 were removed, thus keeping the equivalent β1D residues in the positions found in the X-ray structure of F2-F3 in complex with the cytoplasmic tail of integrin β1D (PDB ID code 3G9W). This resulted in a chimeric structure (β3 residues 688–719/β1D residues 753–787) for the β subunit that combined the TM domain of β3 and the C-terminal tail of β1D. We note that the TM domains of β3 and β1D are very similar in sequence (90% similarity; 52% identity) and that the crucial salt bridge in the IMC, between β1D D759 and αIIb R995, is preserved.

To explore the stability of the IMC αIIb R995/β1D D759 salt bridge in this model of αβ-F2-F3, four atomistic simulations, each of 20-ns duration, were performed for the model in a POPC/POPG bilayer. Rapid rearrangement of the salt bridge was observed, due to the interactions of the αIIbR995D sidechains with a positively charged loop (residues M322–L328) in the talin F3 subdomain. An additional control was performed, using a second model with a slightly different β chain chimera (β3 residues 688–727/β1D residues 764–787). In this model, the homologous salt bridge is formed between the sidechains of β3 D723 and αIIb R995. A similar rapid reorganization of the salt bridge was again observed in the presence of F2-F3, resulting in interactions of the αIIb R995 with the charged loop (residues M322–L328) on the F3 subdomain.

In order to explore the possibility of longer timescale (>0.1 μs) changes in the conformation of the αβ/F2-F3 complex, a multiscale approach was taken, combining CG simulations to explore longer timescale events with subsequent atomistic MD simulations to refine the resultant models. A CG representation of the αβ/F2-F3 model structure was embedded in a POPC/POPG bilayer using our self-assembly protocol (56). Elastic network model restraints between the αIIb subunit and the β/F2-F3 complex were removed. Five simulations (each of 5 μs) were performed. These simulations suggested that talin F2-F3 destabilizes the αIIb/β dimer; the number of contacts between the αIIb and β helices was greatly reduced at the dimer interface with both the IMC and OMC clasps being disrupted. In particular, the close packing of the two helices via the αIIb Gx_3G motif and the interactions of the αIIbF992, F993 aromatic cluster and the αIIbR995 with the β tail were disrupted. The αIIb helix maintained its orientation perpendicular to the bilayer (tilt angle approximately 10°), whereas the β helix tilt increased (tilt angle approximately 28°).

Analysis of the movements of the β and F2-F3 domains relative to the α TM helix suggests how F2-F3 may perturb the αIIb/β interactions. Each of the three CG simulations showed similar

perturbation of the αIIb/β dimer. (The movements of β, F2, and F3 relative to α are shown in Fig. S1.) A 25° ± 4° rotation of F2 in a plane perpendicular to the bilayer normal (i.e., parallel to the lipid–water interface) is observed, along with a 22° ± 1° rotation of F3 in the same plane. This, in turn, induced a 22° ± 1° rotation of the β subunit perpendicular to the membrane in the same direction as for F3 (Fig. S2). This rotation resulted in disruption of the αIIb/β TM helix dimer interactions in both the IMC and OMC regions and the formation of a new interface between the two helices (see Fig. 3*A*).

Three representative CG structures were selected for detailed investigation by atomistic simulations. The starting structures for the three simulations were: (*i*) αβ-F2F3c-AT, a structure with the IMC and OMC interactions preserved, taken to represent a "closed" (c) model; (*ii*) αβ-F2F3p-AT, a structure with the OMC disrupted but the IMC interaction intact, taken to represent a "partially" (p) disrupted model; and (*iii*) αβ-F2F3o-AT, a structure with both the OMC and IMC disrupted taken to represent an "open" (o) model. All three of these models were converted back to atomistic resolution using our CG2AT protocol (49) and were then subjected to 100-ns simulations (Table 1).

In simulation αβ-F2F3c-AT, the helix dimer was observed to stay closed, but the β helix tilt angle increased to approximately 35° relative to the bilayer normal. This increase in the β TM tilt angle and the preservation of the tight interactions between the TM helices thus increased the αIIb helix tilt angle relative to the bilayer normal to approximately 20°. In simulation αβ-F2F3p-AT, the αIIbR995D-βD759 salt bridge was disrupted but the interactions between the αIIbF992F993 residues and the β tail remained, in good agreement with results from simulations of mutations in the αIIb/β3 dimer, discussed above.

In contrast, simulations based on the open structure, αβ-F2F3o-AT, revealed more complex behavior. The interactions in both the OMC and IMC clasp remained disrupted, and the αIIb/β3 dimer remains destabilized (Fig. 3*B*, *C*). Alignment of the αIIb helix at the start and end of these simulations revealed that the F2 domain had rotated perpendicular to the bilayer normal. This, in turn, causes rotation of F3 in the same plane but in the opposite direction, whereas the β tail rotated in the same direction of F3. Interestingly, the dimer destabilization in αβ-F2F3o-AT allowed further dissociation of the helices in the OMC clasp region. In particular, the distance between the αIIb and the β3 helices in this region is increased to approximately 20 Å, and therefore the angle between the two TM helices also increased. However, the IMC region remained relatively intact, and thus a "scissor" movement of the two helices was observed, with the center of the scissor in the region of the IMC. The new interface in this contact region involves αIIb L978, L979, I982, A986, V990 and the β I707, G708, A711, T715, M718 residues (see Fig S3).

We note that during these movements the interactions of the F2-F3 and of the β C-terminal tail with the bilayer were preserved. In particular, the F2-F3 domains interacted preferentially with the negatively charged lipids in the membrane. This suggests that protein/lipid interactions must be considered when analyzing possible activation mechanisms of integrins.

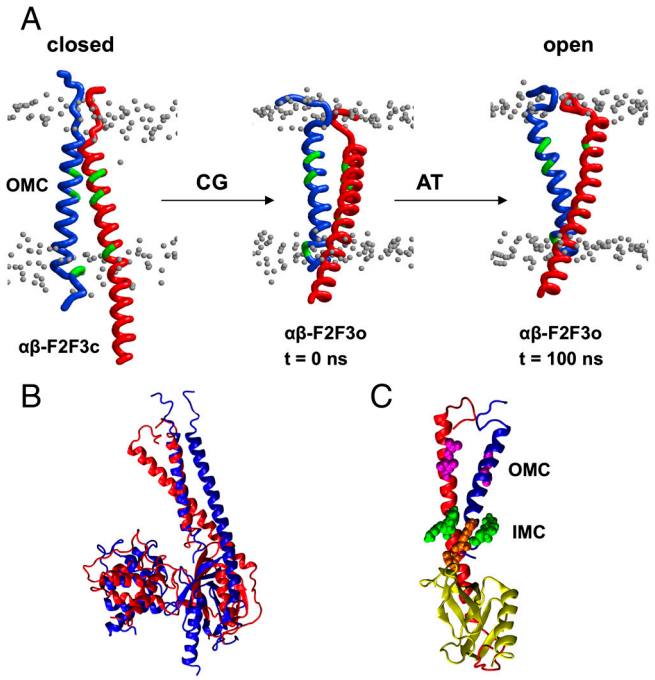

Fig. 3. Simulations of the αIIbβ3 TM helix dimer in complex with talin F2-F3. (*A*) Movements of the α and β TM domains in the αβ-F2F3-AT simulations. Three structures are shown: the closed structure at the start of the CG-MD simulations (αβ-F2F3c-AT), a representative structure from the open cluster after the CG-MD simulations (αβ-F2F3o-AT), and the final open structure from 100-ns AT-MD simulation. In these diagrams, only the Cα traces of the TM helices (α in blue; β in red) are shown, along with the phosphorus atoms of the nearby lipid headgroups (gray). The OMC residues and the aromatic residues of the IMC are shown in green. (*B*) Initial (blue) and final ($t = 100$ ns; red) configuration of the αβ-F2-F3 complex in the αβ-F2F3o-AT simulation. The αIIb TM helix from the initial and the final structures of the simulation are superimposed. (*C*) Snapshot corresponding to the final ($t = 100$ ns) configuration of the αβ-F2F3o-AT simulation showing that the interactions in both the IMC and the OMC are disrupted. The F2 subdomain of talin is omitted for clarity.

Suggested Mechanism. Structural studies (7, 14, 16, 24, 25, 57) have greatly increased our understanding of integrin activation from inside the cell. However, static structures fall short of revealing dynamic mechanisms of activation. Using multiscale MD simulations, we have revealed further details of the mechanism whereby the talin head domain, the lipid bilayer membrane and the α/β TM helix dimer together interact to enable inside-out activation of integrins. In particular, we propose a mechanism whereby talin F2-F3 interactions lead to a conformational change in the αβ TM helix dimer, which may act as a trigger for inside-out activation of the integrin ectodomain. In this model (see Fig. 4*A*) the first stage is when F2-F3 binds to anionic lipids via electrostatic interactions (18). This is determined by the F2 subdomain, which forms basic sidechain/anionic headgroup interactions. Talin F3 binds to the β integrin C-terminal tail in three areas: the membrane distal NPxY motif, the β1D W775 (β3 W739) residue, and the β tail membrane-proximal region. Previous experimental studies have shown that a tyrosine to alanine mutation in the distal NPxY motif or the β3 R358A mutation inhibits integrin activation (7, 8, 58–60). Thus, F2-F3 associates with the α/β TM helix dimer via an interaction between F3 and the cytoplasmic tail of β. A recent NMR study (61) suggested that, in the resting integrin off state, the β TM region is bent at residue R724, allowing the C-terminal cytoplasmic β tail to interact with the membrane via two helices. Promotion of a helical structure in the R724 region would extend the β helix and allow binding of F3. This, together with F2-F3 interactions with the membrane bilayer, then leads to a scissoring motion of the α/β TM helix dimer about the IMC such that the OMC is disrupted, and the N-termini (extracellular) separation of the TM helices is increased (Fig. 3*A*, Dataset S1, and Dataset S2).

The scissoring motion that was revealed in the αβF2F3o-AT simulations reflects the tendency of the β TM helix to be more tilted in a lipid bilayer than it is in the off state. This tilting motion may be seen quite clearly by monitoring the distances between the α and β TMs. As shown in Fig. 4 *A* and *B*, distances in the IMC region (d3, d4) are maintained, whereas the distances (d1, d2) at the N termini of the helices increase by about 6 Å from start to end of the simulation.

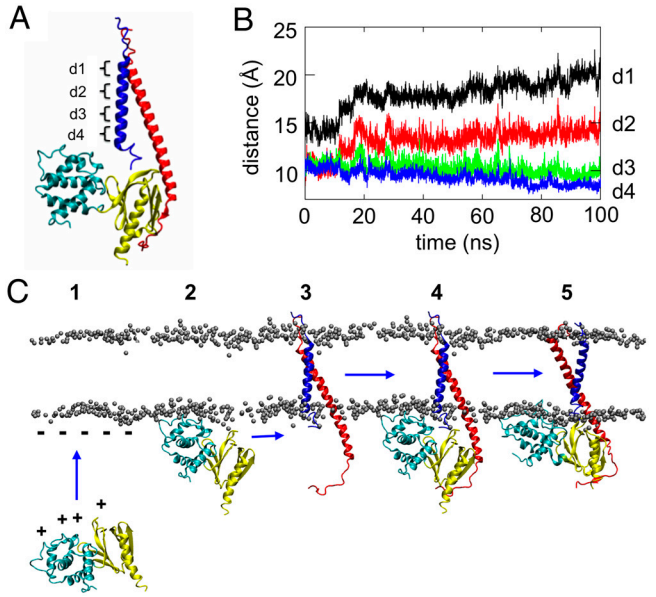

Fig. 4. (*A*) Proposed mechanism of integrin inside-out activation. The positively charged patch on the F2 and F3 subdomains of talin (1) interacts with the negatively charged headgroups on the membrane surface (2), orienting talin for binding to the β cytoplasmic tail (3). Upon talin binding (4), the αIIbR995-β3D723 salt bridge is disrupted because of the interactions of the αIIbR995 with the talin F3 acidic loop. Strengthening of interactions between the positively charged surface patch of F2 and the membrane surface rotates the talin F2 subdomain approximately 34° in a plane perpendicular to the bilayer normal (i.e., parallel to the lipid–water interface). This in turn rotates F3 (approximately 26°) and the β tail (approximately 30°) in the opposite direction and in the same plane. This, in combination with an approximately 15° increase in the tilt angle of the β helix relative to the bilayer normal, disrupts the interactions in both the IMC and the OMC of the αβ dimer (5). This is suggested to promote a switch of the integrin ectodomain to an active extended state. *B* and *C* illustrate the proposed scissors motion of the integrin α and β TM helices that occurs on activation by talin. *B* indicates four interhelix distances (d1 to d4) that characterize the scissors motion, and *C* shows the time evolution of d1 to d4 over the course of one of the three αβ-F2F3o-AT simulations.

We have used the coordinates of the αIIb/β3 structure determined by NMR in bicelles (PDB ID code 2K9J) here. Other structures have been reported, determined either in organic solvents (PDB ID code 2KNC) (25, 27) or from computational approaches (26, 62). In 2KNC, which was obtained using a 1:1 mixture of acetonitrile and water, the IMC part is different from both 2K9J and the computational models, suggesting that the lipid environment is important for the formation of the IMC interactions. It is of interest, however, that 2KNC is rather like αβF2-F3p, suggesting that it might relate to an intermediate state between off and on (Fig. S4).

The scissor model for inside-out activation of integrins suggests how the integrin ectodomain might be stimulated to go from a bent inactive state to an extended active state (34–36). Talin weakens αIIb/β3 interactions, thus promoting a scissor movement of the TM part of the two helices with a perturbed IMC as the center of the scissor movement. This is in agreement with the recent suggestion that disruption of the α/β dimer involves competition between an α/β tail salt bridge and a talin/β tail salt bridge as well as a 20° reorientation of the β integrin tail in a plane perpendicular to the membrane There is ample experimental data to suggest that OMC and IMC interactions are required for integrin activation (23–25, 30–32, 53, 63–66). Our results have clarified the role of the IMC and OMC clasps and explain much of the experimental data. Deletion or mutation of residues in the GFFKR motif in the α tail lead to integrin activation (30, 40, 65, 66). Similarly, deletion of the β tail cytoplasmic region leads to activation (39, 64). Further, leucine or isoleucine mutations in the GxxxG motif in the OMC clasp cause steric clashes and thus disruption of the packing of the α/β dimer (24, 31, 53). Our results are also in good agreement with mutational experimental results that suggest that disruption of the F3/ β tail interface or on the talin F2-F3 interface with the membrane reduce the ability of talin to activate integrins (7–14). Fluorescent resonance energy transfer (FRET) studies (29) using αL and β2 integrin subunits tagged with fluorescent proteins suggested significant reduction in the FRET signal in the presence of talin, and this was interpreted in terms of tail separation. A scissor movement around the IMC might be expected to separate the scissor handles as well as the blades. Fig 4*B* (d4) does not indicate an increase in separation, but the αIIbR995-β3D723R is broken and the largely cytoplasmic α and β tails are flexible, so increased tail separation is not inconsistent with our model.

Recent structures of integrin ectodomains shows that the membrane-proximal C-terminal regions of the two ectodomain subunits are in close proximity (26, 36, 67). It is therefore plausible that the scissor movement that causes dissociation of the OMC clasp promotes a rearrangement of the integrin ectodomain.

In summary, our results suggest a mechanism for integrin inside-out activation that explains the role of the talin head domain, the membrane and the α/β TM interactions. We have shown that the α/β TM helix dimer is conformationally stable in a lipid bilayer on a 100-ns timescale, that the β TM helix has a propensity to tilt relative to the lipid bilayer and that this tilt motion is resisted by the presence of the α TM helix. Binding of talin destabilizes interactions between the TM helices and permits a scissor-like motion in part driven by the propensity of the β helix to tilt. This model shows how protein/membrane interactions can disrupt the TM helix interactions of complex receptors and potentially lead to structural changes in ectodomains. It also demonstrates the strength of multiscale simulations for developing models of the conformational dynamics of a complex membrane receptor.

Materials and Methods

CG-MD Simulations. CG-MD simulations were performed using a local variant (68) of the Martini force field (69) with an elastic network applied to backbone particles using a cutoff distance of 7 Å, and the protein inserted in a POPC/POPG bilayer. The system was solvated, energy minimized for 200 steps, and equilibrated for 5 ns with the protein backbone particle restrained. After that, five production simulations were carried out for 5 μs each.

All CG-MD simulations were performed using GROMACS 3.3.3 (www.gromacs.org) (70, 71). A Berendsen thermostat (72) (coupling constant of 1.0 ps; reference temperature 310 K) and barostat (coupling constant of 1.0 ps; compressibility value of 5.0×10^{-6} bar^{-1}; reference pressure 1 bar) were used. The integration time step was 40 fs. Lennard–Jones and Coulombic interactions were shifted to zero between 9 and 12 Å, and 0 and 12 Å, respectively. CG to atomistic conversion used a fragment-based approach (49).

Atomistic MD Simulations. Atomistic MD simulations were performed using the GROMOS96 43a1 force field (73). The Parinello–Rahman barostat (74) and Berendsen thermostat (72). The LINCS algorithm was used to constrain bond lengths (75), and particle mess Ewald particle mesh was used to model electrostatics up to 10 Å. A 10-Å cutoff distance was also used for van der Waals interactions. Systems were equilibrated for 2 to 5 ns with the protein Cα atoms restrained, followed by unrestrained MD simulations as in Table 1. Analyses used Gromacs, VMD (76), and locally written codes.

ACKNOWLEDGMENTS. This research was funded by the Wellcome Trust. I.D.C. acknowledges support from the National Institutes of Health Cell Migration consortium.

1. Wegener KL, Campbell ID (2008) Transmembrane and cytoplasmic domains in integrin activation and protein-protein interactions (review). *Mol Membr Biol* 25:376–387.

2. Hynes RO (2002) Integrins: Bidirectional, allosteric signaling machines. *Cell* 110:673–687.

3. Ginsberg MH, Partridge A, Shattil SJ (2005) Integrin regulation. *Curr Opin Cell Biol* 17:509–516.
4. Harburger DS, Calderwood DA (2009) Integrin signalling at a glance. *J Cell Sci* 122:159–163.
5. Bennett JS, Berger BW, Billings PC (2009) The structure and function of platelet integrins. *J Thromb Haemost* 7:200–205.
6. Gong H, et al. (2010) G Protein subunit $G\alpha_{13}$ binds to integrin $\alpha_{IIb}\beta_3$ and mediates integrin "outside-in" signaling. *Science* 327:340–343.
7. Wegener KL, et al. (2007) Structural basis of integrin activation by talin. *Cell* 128:171–182.
8. Tadokoro S, et al. (2003) Talin binding to integrin β tails: A final common step in integrin activation. *Science* 302:103–106.
9. Petrich BG, et al. (2007) Talin is required for integrin-mediated platelet function in hemostasis and thrombosis. *J Exp Med* 204:3103–3111.
10. Calderwood DA, et al. (1999) The talin head domain binds to integrin β subunit cytoplasmic tails and regulates integrin activation. *J Biol Chem* 274:28071–28074.
11. Ulmer TS, Calderwood DA, Ginsberg MH, Campbell ID (2003) Domain-specific interactions of talin with the membrane-proximal region of the integrin β3 subunit. *Biochemistry* 42:8307–8312.
12. Bouaouina M, Lad Y, Calderwood DA (2008) The N-terminal domains of talin cooperate with the phosphotyrosine binding-like domain to activate β1 and β3 Integrins. *J Biol Chem* 283:6118–6125.
13. Calderwood DA (2004) Talin controls integrin activation. *Biochem Soc Trans* 32:434–437.
14. Anthis NJ, et al. (2009) The structure of an integrin/talin complex reveals the basis of inside-out signal transduction. *EMBO J* 28:3623–3632.
15. Critchley DR, Gingras AR (2008) Talin at a glance. *J Cell Sci* 121:1345–1347.
16. Elliott PR, et al. (2010) The structure of the talin head reveals a novel extended conformation of the FERM domain. *Structure* 18:1289–1299.
17. Calderwood DA, et al. (2002) The phosphotyrosine binding-like domain of talin activates integrins. *J Biol Chem* 277:21749–21758.
18. Kalli AC, et al. (2010) The structure of the talin/integrin complex at a lipid bilayer: An NMR and MD simulation study. *Structure* 18:1280–1288.
19. Saltel F, et al. (2009) New PI(4,5)P_2- and membrane proximal integrin-binding motifs in the talin head control β3-integrin clustering. *J Cell Biol* 187:715–731.
20. Goult BT, et al. (2010) Structure of a double ubiquitin-like domain in the talin head: A role in integrin activation. *EMBO J* 29:1069–1080.
21. Adair BD, Yeager M (2002) Three-dimensional model of the human platelet integrin $\alpha_{IIb}\beta_3$ based on electron cryomicroscopy and X-ray crystallography. *Proc Natl Acad Sci USA* 99:14059–14064.
22. Schneider D, Engelman DM (2004) Involvement of transmembrane domain interactions in signal transduction by α/β integrins. *J Biol Chem* 279:9840–9846.
23. Luo B-H, Springer TA, Takagi J (2004) A specific interface between integrin transmembrane helices and affinity for ligand. *PLoS Biol* 2:e153.
24. Lau TL, Kim C, Ginsberg MH, Ulmer TS (2009) The structure of the integrin αIIbβ3 transmembrane complex explains integrin transmembrane signalling. *EMBO J* 28:1351–1361.
25. Yang J, et al. (2009) Structure of an integrin αIIbβ3 transmembrane-cytoplasmic heterocomplex provides insight into integrin activation. *Proc Natl Acad Sci USA* 106:17729–17734.
26. Zhu J, et al. (2009) The structure of a receptor with two associating transmembrane domains on the cell surface: Integrin $\alpha_{IIb}\beta_3$. *Mol Cell* 34:234–249.
27. Vinogradova O, et al. (2002) A structural mechanism of integrin αIIbβ3 "inside-out" activation as regulated by its cytoplasmic face. *Cell* 110:587–597.
28. Bhunia A, et al. (2009) NMR solution conformations and interactions of integrin αLβ2 cytoplasmic tails. *J Biol Chem* 284:3873–3884.
29. Kim M, Carman CV, Springer TA (2003) Bidirectional transmembrane signaling by cytoplasmic domain separation in integrins. *Science* 301:1720–1725.
30. Hughes PE, et al. (1996) Breaking the integrin hinge: A defined structural constraint regulates integrin signaling. *J Biol Chem* 271:6571–6574.
31. Li W, et al. (2005) A push-pull mechanism for regulating integrin function. *Proc Natl Acad Sci USA* 102:1424–1429.
32. Partridge AW, et al. (2005) Transmembrane domain helix packing stabilizes integrin αIIbβ3 in the low affinity state. *J Biol Chem* 280:7294–7300.
33. Zhu JQ, et al. (2007) Requirement of alpha and beta subunit transmembrane helix separation for integrin outside-in signaling. *Blood* 110:2475–2483.
34. Adair BD, et al. (2005) Three-dimensional EM structure of the ectodomain of integrin αVβ3 in a complex with fibronectin. *J Cell Biol* 168:1109–1118.
35. Rocco M, et al. (2008) Integrin conformational regulation: Uncoupling extension/tail separation from changes in the head region by a multiresolution approach. *Structure* 16:954–964.
36. Zhu JH, et al. (2008) Structure of a complete integrin ectodomain in a physiologic resting state and activation and deactivation by applied forces. *Mol Cell* 32:849–861.
37. Nogales A, et al. (2010) Three-dimensional model of human platelet integrin αIIbβ3 in solution obtained by small angle neutron scattering. *J Biol Chem* 285:1023–1031.
38. Williams MJ, Hughes PE, O'Toole TE, Ginsberg MH (1994) The inner world of cell adhesion: Integrin cytoplasmic domains. *Trends Cell Biol* 4:109–112.
39. Lu C, Takagi J, Springer TA (2001) Association of the membrane proximal regions of the α and β subunit cytoplasmic domains constrains an integrin in the inactive state. *J Biol Chem* 276:14642–14648.
40. Luo B-H, Carman CV, Springer TA (2007) Structural basis of integrin regulation and signaling. *Annu Rev Immunol* 25:619–647.
41. Adcock SA, McCammon JA (2006) Molecular dynamics: Survey of methods for simulating the activity of proteins. *Chem Rev* 106:1589–1615.
42. Ash WL, Zlomislic MR, Oloo EO, Tieleman DP (2004) Computer simulations of membrane proteins. *Biochim Biophys Acta* 1666:158–189.
43. Psachoulia E, Marshall D, Sansom MSP (2010) Molecular dynamics simulations of the dimerization of transmembrane α-helices. *Acc Chem Res* 43:388–396.
44. Liepina I, Czaplewski C, Janmey P, Liwo A (2003) Molecular dynamics study of a gelsolin-derived peptide binding to a lipid bilayer containing phosphatidylinositol 4,5-bisphosphate. *Biopolymers* 71:49–70.
45. Jaud S, Tobias DJ, Falke JJ, White SH (2007) Self-induced docking site of a deeply embedded peripheral membrane protein. *Biophys J* 92:517–524.
46. Psachoulia E, Sansom MSP (2008) Interactions of the pleckstrin homology domain with phosphatidylinositol phosphate and membranes: Characterization via molecular dynamics simulations. *Biochemistry* 47:4211–4220.
47. Psachoulia E, Sansom MSP (2009) PX and FYVE mediated interactions with membranes: Simulation studies. *Biochemistry* 48:5090–5095.
48. Ayton GS, Voth GA (2009) Systematic multiscale simulation of membranes protein systems. *Curr Opin Struct Biol* 19:138–144.
49. Stansfeld PJ, Sansom MSP (2011) From coarse-grained to atomistic: A serial multi-scale approach to membrane protein simulations. *J Chem Theory Comput* 7:1157–1166.
50. Lau T-L, Dua V, Ulmer TS (2008) Structure of the integrin αIIb transmembrane segment. *J Biol Chem* 283:16162–16168.
51. Kim C, Lau TL, Ulmer TS, Ginsberg MH (2009) Interactions of platelet integrin α_{IIb} and β_3 transmembrane domains in mammalian cell membranes and their role in integrin activation. *Blood* 113:4747–4753.
52. MacKenzie KR, Prestegard JH, Engelman DM (1997) A transmembrane helix dimer: Structure and implications. *Science* 276:131–133.
53. Luo B-H, Carman CV, Takagi J, Springer TA (2005) Disrupting integrin transmembrane domain heterodimerization increases ligand binding affinity, not valency or clustering. *Proc Natl Acad Sci USA* 102:3679–3684.
54. Psachoulia E, Bond PJ, Fowler PW, Sansom MSP (2008) Helix-helix interactions in membrane proteins: Coarse grained simulations of glycophorin helix dimerization. *Biochemistry* 47:10503–105012.
55. Lau T-L, Partridge AW, Ginsberg MH, Ulmer TS (2008) Structure of the integrin β3 transmembrane segment in phospholipid bicelles and detergent micelles. *Biochemistry* 47:4008–4016.
56. Scott KA, et al. (2008) Coarse-grained MD simulations of membrane protein-bilayer self-assembly. *Structure* 16:621–630.
57. Goult BT, et al. (2009) The structure of an interdomain complex that regulates talin activity. *J Biol Chem* 284:15097–15106.
58. O'Toole TE, Ylanne J, Culley BM (1995) Regulation of integrin affinity states through an NPXY motif in the β subunit cytoplasmic domain. *J Biol Chem* 270:8553–8558.
59. Garcia-Alvarez B, et al. (2003) Structural determinants of integrin recognition by talin. *Mol Cell* 11:49–58.
60. Ulmer TS, Yaspan B, Ginsberg MH, Campbell ID (2001) NMR analysis of structure and dynamics of the cytosolic tails of integrin αIIb β3 in aqueous solution. *Biochemistry* 40:7498–7508.
61. Metcalf DG, et al. (2010) NMR analysis of the αIIb β3 cytoplasmic interaction suggests a mechanism for integrin regulation. *Proc Natl Acad Sci USA* 107:22481–22486.
62. Metcalf DG, Kulp DW, Bennett JS, DeGrado WF (2009) Multiple approaches converge on the structure of the integrin αIIb/β3 transmembrane heterodimer. *J Mol Biol* 392:1087–1101.
63. Berger BW, et al. (2010) Consensus motif for integrin transmembrane helix association. *Proc Natl Acad Sci USA* 107:703–708.
64. Hughes PE, et al. (1995) The conserved membrane-proximal region of an integrin cytoplasmic domain specifies ligand binding affinity. *J Biol Chem* 270:12411–12417.
65. O'Toole TE, et al. (1994) Integrin cytoplasmic domains mediate inside-out signal-transduction. *J Cell Biol* 124:1047–1059.
66. O'Toole TE, et al. (1991) Modulation of the affinity of integrin $\alpha_{IIb}\beta_3$ (GpIIb-IIIa) by the cytoplasmic domain of α_{IIb}. *Science* 254:845–847.
67. Xiong JP, et al. (2009) Crystal structure of the complete integrin αVβ3 ectodomain plus an α/β transmembrane fragment. *J Cell Biol* 186:589–600.
68. Bond PJ, Wee CL, Sansom MSP (2008) Coarse-grained molecular dynamics simulations of the energetics of helix insertion into a lipid bilayer. *Biochemistry* 47:11321–11331.
69. Monticelli L, et al. (2008) The MARTINI coarse grained force field: Extension to proteins. *J Chem Theory Comput* 4:819–834.
70. Lindahl E, Hess B, van der Spoel D (2001) GROMACS 3.0: A package for molecular simulation and trajectory analysis. *J Mol Model* 7:306–317.
71. van der Spoel D, et al. (2005) GROMACS: Fast, flexible, and free. *J Comput Chem* 26:1701–1718.
72. Berendsen HJC, et al. (1984) Molecular dynamics with coupling to an external bath. *J Chem Phys* 81:3684–3690.
73. Scott WRP, et al. (1999) The GROMOS biomolecular simulation program package. *J Phys Chem A* 103:3596–3607.
74. Parrinello M, Rahman A (1981) Polymorphic transitions in single-crystals-a new molecular-dynamics method. *J Appl Phys* 52:7182–7190.
75. Hess B, Bekker H, Berendsen HJC, Fraaije JGEM (1997) LINCS: A linear constraint solver for molecular simulations. *J Comput Chem* 18:1463–1472.
76. Humphrey W, Dalke A, Schulten K (1996) VMD–Visual molecular dynamics. *J Mol Graph* 14:33–38.